Di- and Trinuclear Complexes with the Mono- and Dianion of 2,6-Bis(phenylamino)pyridine: High-Field Displacement of Chemical Shifts Due to the Magnetic Anisotropy of Quadruple Bonds

F. Albert Cotton,*,† Lee M. Daniels,† Peng Lei,† Carlos A. Murillo,*,†,‡ and Xiaoping Wang†

Department of Chemistry and Laboratory for Molecular Structure and Bonding, P.O. Box 30012, Texas A&M University, College Station, Texas 77842-3012, and Department of Chemistry, University of Costa Rica, Ciudad Universitaria, Costa Rica

Received December 6, 2000

The monoanion of 2,6-bis(phenylamino)pyridine ($HBPAP^-$) has been found to support quadruply bonded Cr_2^{4+} and Mo_2^{4+} units in $Cr_2(HBPAP)_4$ (**1**) and $Mo_2(HBPAP)_4$ (**2**). The corresponding dianion $BPAP^{2-}$ was able to stabilize the trinuclear complexes, $(TBA)_2Cr_3(BPAP)_4$ (**3**) and $(TBA)_2Ni_3(BPAP)_4$ (**4**), where TBA is the tetrabutylammonium cation. The dinuclear complexes have the typical paddlewheel configuration with Cr−Cr distances of about 1.87 Å and a Mo−Mo distance of 2.0813(5) Å and exhibit a high-field displacement of the corresponding N−H signals caused by the magnetic anisotropy of the quadruple bonds. For the trinuclear complexes, **3** has a linear chain of three chromium atoms arranged in an unsymmetrical fashion with two chromium atoms paired to give a quadruply bonded unit (Cr−Cr distance: 1.904(3) Å) and an isolated, square planar Cr^{II} unit at 2.589(3) Å from the dimetal unit. On the other hand, the three nickel atoms in **4** are evenly spaced, having Ni···Ni distances of 2.3682(8) Å. The trinuclear compounds show a twisted conformation with an overall torsion angle of about 30°.

Introduction

Growing attention has been given to the preparation and study of compounds having linear chains of metal atoms surrounded by four ligands, both in our laboratory[1] and elsewhere.[2] So far, linear chains with up to nine atoms have been reported.[3] Studies from our group on the trinuclear dpa complexes,[1,4] where dpa stands for the anion of di(2-pyridyl)amine, have shown that the behavior of the trinuclear systems is far more complicated than one might have expected. Specifically, both symmetrical and unsymmetrical chains can occur[1,4] and interpretation of the magnetic behavior of certain complexes such as $Co_3(dpa)_4XY$ has been a challenging task;[1,4] here X and Y are mononuclear anions such as BF_4^-,[5] CN^-,[1h] $N(CN)_2^-$,[1h] Cl^-,[1e] Br^-,[1g] and SCN^-.[1h] We believe that only after a better understanding of the simplest trinuclear systems is obtained could we hope to make progress in the preparation of molecular wires, an important goal of the study of linear metal chain systems.

In all known $M_3(dpa)_4X_2$ compounds (M = Cr,[1d] Co,[1e] Ni,[1f,2e] Cu,[2e] Ru,[2d] and Rh[2d]), the dpa anion is not planar because of the repulsion of two hydrogen atoms on different, but adjacent pyridine rings shown in Scheme 1a. This leads a considerable torsion angle and a helical arrangement of the four dpa ligands around the trimetal unit as shown in Scheme 2. The configuration can be of either right- or left-handed helicity; chiral crystals containing only one of the two configurations have been isolated.[6] To avoid the H···H repulsion and thus obtain a flat ligand that will not demand a helical conformation in the product, another tridentate ligand having free rotation of two terminal aromatic rings was considered desirable. We have prepared one such ligand, namely, 2,6-bis(phenylamino)pyridine, H_2BPAP, shown in Scheme 1b. Moreover, since a recent study in our group had shown that electron-donating atoms in appended groups near the axial positions of a dichromium core can greatly affect the Cr−Cr distance,[7] we felt that preparing dinuclear complexes with this tridentate ligand could also be of interest. Finally, since the BPAP ligand is a dianion, the resulting trimetal complexes, $M_3(BPAP)_4^{2-}$, must be anionic

* To whom correspondence should be addressed. E-mail: cotton@tamu.edu; murillo@tamu.edu.

† Texas A&M University.

‡ University of Costa Rica.

(1) See, for example: (a) Cotton, F. A.; Daniels, L. M.; Murillo, C. A.; Wang, X. *Chem. Commun.* **1998**, 39. (b) Clérac, R.; Cotton, F. A.; Daniels, L. M.; Dunbar, K. R.; Murillo, C. A.; Pascual, I. *Inorg. Chem.* **2000**, *39*, 752. (c) Clérac, R.; Cotton, F. A.; Dunbar, K. R.; Lu, T.; Murillo, C. A.; Wang, X. *J. Am. Chem. Soc.* **2000**, *122*, 2272. (d) Cotton, F. A.; Daniels, L. M.; Murillo, C. A.; Pascual, I. *J. Am. Chem. Soc.* **1997**, *119*, 10223. (e) Cotton, F. A.; Daniels, L. M.; Jordan, G. T., IV. *Chem. Commun.* **1997**, 421. (f) Clérac, R.; Cotton, F. A.; Dunbar, K. M.; Murillo, C. A.; Pascual, I.; Wang, X. *Inorg. Chem.* **1999**, *38*, 2655. (g) Clérac, R.; Cotton, F. A.; Daniels, L. M.; Dunbar, K. M.; Murillo, C. A.; Wang, X. *J. Chem. Soc., Dalton Trans.* **2001**, 386. (h) Clérac, R.; Cotton, F. A.; Jeffery, S. P.; Murillo, C. A.; Wang, X. *Inorg. Chem.* **2001**, *40*, 1265.

(2) (a) Shieh, S. J.; Chou, C. C.; Lee, G. H.; Wang, C. C.; Peng, S. M. *Angew. Chem., Int. Ed. Engl*. **1997**, *36*, 56. (b) Wang, C. C.; Lo, W. C.; Chou, C. C.; Lee, G. H.; Chen, J. M.; Peng, S. M. *Inorg. Chem.* **1998**, *37*, 4059. (c) Pyrka, G. J.; El-Mekki, M.; Pinkerton, A. A. *J. Chem. Soc., Chem. Commun.* **1991**, 84. (d) Sheu, J. T.; Lin, C. C.; Chao, I.; Wang, C. C.; Peng, S. M. *Chem. Commun.* **1996**, 315. (e) Adulchecha, S.; Hathaway, B. *J. Chem. Soc., Dalton Trans.* **1991**, 993.

(3) (a) Chen, Y. H.; Lee, C. C.; Wang, C. C.; Lee, G. H.; Lai, S. Y.; Li, F. Y.; Mou, C. Y.; Peng, S. M. *Chem. Commun*. **1999**, 1667. (b) Peng, S. M.; Wang, C. C.; Jang, Y. L.; Chen, Y. H.; Li, F. Y.; Mou, C. Y.; Leung, M. K. *J. Magn. Magn. Mater.* **2000**, *209*, 80.

(4) Cotton, F. A. *Inorg. Chem.* **1998**, *37*, 5710.

(5) Cotton, F. A.; Daniels, L. M.; Jordan IV, G. T.; Murillo, C. A. *J. Am. Chem. Soc.* **1997**, *119*, 10377.

(6) Clérac, R.; Cotton, F. A.; Dunbar, K. R.; Lu, T.; Murillo, C. A.; Wang, X. *Inorg. Chem.* **2000**, *39*, 3065.

(7) Cotton, F. A.; Daniels, L. M.; Murillo, C. A.; Pascual, I.; Zhou, H. *J. Am. Chem. Soc.* **1999**, *121*, 6856.

10.1021/ic001376g CCC: $20.00
Published on Web 05/01/2001

Scheme 1

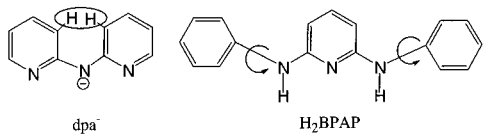

Scheme 2

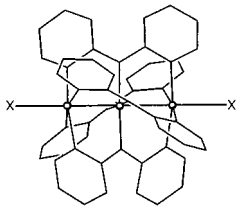

when M is a divalent ion and would not therefore be expected to have axial anionic ligands. We hoped, therefore, to see if the absence of axial ligands would have a significant effect on the electronic structure of the trimetal chain.

Here we report the preparation and structural characterization of four species, two dinuclear and two trinuclear. They are $Cr_2(HBPAP)_4$ (**1**), $Mo_2(HBPAP)_4$ (**2**), $(Bu^n{}_4N)_2Cr_3(BPAP)_4$ (**3**), and $(Bu^n{}_4N)_2Ni_3(BPAP)_4$ (**4**).

Experimental Section

General Procedures. All manipulations were carried out under nitrogen using standard Schlenk techniques. Solvents were dried by conventional methods and were freshly distilled under nitrogen before use. Anhydrous $CrCl_2$ and $NiCl_2$, as well as 2,6-dibromopyridine, were purchased from Strem Chemicals and stored in a N_2 drybox; MeLi, $Bu^n{}_4NBr$, and aniline hydrochloride were purchased from Aldrich and used as received; $Mo_2(O_2CCF_3)_4$ was prepared as reported earlier.[8] The ^1H NMR spectra were recorded on a Varian XL-300 instrument at 300 MHz. Cyclic voltammetry was performed in dichloromethane for compound **1** and in THF for compound **3** with a BAS model 100 scanning potentiostat using Pt working and auxiliary electrodes and 0.1 M TBAH ($Bu^n{}_4NPF_6$) as the supporting electrolyte. Potentials are referenced to the ferrocene/ferrocenium (Fc/Fc^+) couple, which occurs at $E_{1/2} = +0.44$ V versus Ag/AgCl. The values of $E_{1/2}$ were taken as $(E_{pa} + E_{pc})/2$, where E_{pa} and E_{pc} are the anodic and cathodic peak potentials, respectively, for the quasireversible peaks. Elemental analyses were performed by Canadian Microanalytical Service Ltd.

Preparation of 2,6-Bis(phenylamino)pyridine. This was prepared according to the literature[9] with some modifications: 2,6-dibromopyridine (12.5 g, 50.0 mmol) and aniline hydrochloride (23.5 g, 250 mmol) were added to a 500 mL three-neck flask fitted with a stirring bar and a condenser. The mixture was heated to 200 °C. As the mixture melted, it turned dark orange. After 4 h of stirring under N_2, 100 mL of aqueous 10% sodium carbonate solution was added to the mixture to neutralize the acid. Chloroform (2×150 mL) was added to extract the product from the aqueous solution. The volume was reduced to ca. 40 mL under reduced pressure, and then 100 mL of ethanol was added. Further addition of a large amount of water into the $EtOH/CHCl_3$ solution precipitated a yellow product, which was recrystallized twice from water−ethanol and then from an ethyl acetate−hexanes mixture. Yield: 16.5 g (65%, based on 2,6-dibromopyridine). Anal. Calcd for $C_{17}N_3H_{15}$: C, 78.16; H, 5.75; N, 16.09. Found: C, 78.11; H, 5.70; N, 16.02. ^1H NMR (300 MHz, CD_2Cl_2, δ): 8.04 (broad, 2H), 7.63 (d, 4H), 7.45 (t, 1H), 7.20 (t, 4H), 6.88 (t, 2H), 6.28 (d, 2H).

Preparation of Li(HBPAP). Methyllithium (1.05 mmol) was added to a 15 mL THF solution containing H_2BPAP (0.267 g, 1.00 mmol) at −78 °C. After the THF solution was allowed to warm up slowly to room temperature, the volume was reduced to ca. 7 mL and some yellow precipitate formed. Addition of 35 mL of hexanes increased the amount of solid. This was collected by filtration, washed with 10 mL of hexanes, and then dried under vacuum. Yield: 0.256 g (95%). ^1H NMR (300 MHz, CD_2Cl_2, δ): 7.38 (d, 4H), 7.29 (m, 5H), 7.02 (t, 2H), 6.44 (broad, 1H), 6.31 (d, 2H).

Preparation of 1·toluene and 1·C_6H_{14}. The compound H_2DPAP (0.522 g, 2.00 mmol) was dissolved in 15 mL of THF and then deprotonated by adding MeLi (2.1 mmol) at −78 °C. The THF solution was allowed to return slowly to room temperature and transferred into a flask containing $CrCl_2$ (0.135 g, 1.10 mmol). After the mixture was stirred at room temperature overnight, a red orange solid formed and was separated by filtration. This solid was found to be slightly soluble in toluene and dichloromethane. To the solid was added 20 mL of toluene, and the mixture was filtered. Then a layer of hexanes was added to the toluene solution. After 2 weeks, crystals of **1**·toluene suitable for X-ray studies formed. The filtrate from the original mixture was dried under vacuum. The solid was washed with ether, 2×20 mL; it was dissolved in THF, and the solution was layered with hexanes. Red crystals of **1**·C_6H_{14} suitable for X-ray study were obtained after 9 days. The overall yield was 0.430 g (87%). ^1H NMR (300 MHz, CD_2Cl_2, δ): 7.23 (m, 12H), 7.02 (m, 12H), 6.75 (m, 12H), 5.95 (d, 4H), 6.78 (t, 12H), 3.4 (d, 4H). Anal. Calcd for $C_{68}H_{56}N_{12}Cr_2$: C, 71.32; H, 4.92; N, 14.68. Found: C, 70.75; H, 5.11; N, 14.44. CV: one quasireversible wave at 0.32 V in the scan range 0.00 to +0.06 V and two irreversible waves at 0.38 and 0.86 V in the scan range 0.00 to +1.00 V.

Preparation of 2·toluene. The ligand precursor H_2BPAP (0.522 g, 2.00 mmol) was dissolved in 15 mL of THF and deprotonated with 1 equiv of MeLi at −78 °C. After the temperature of the solution had slowly risen to room temperature, the solution was added to a flask containing $Mo_2(O_2CCF_3)_4$ (0.32 g, 0.50 mmol). The reaction mixture was stirred overnight, and the solvent was then removed under vacuum. The remaining solid was washed with 2×20 mL of hexanes, then dissolved in toluene, and layered with hexanes. Red crystals suitable for X-ray study were obtained after 2 weeks. Yield: 0.320 *g* (78%). ^1H NMR (300 MHz, CD_2Cl_2, δ): 7.43 (d, 16H), 7.40 (t, 4H), 7.35 (t, 16H), 7.05 (t, 8H), 6,34 (d, 8H), 3.04 (broad, 4H). Anal. Calcd for $C_{68}H_{56}N_{12}Mo_2$: C, 66.23; H, 4.58; N, 13.63. Found: C, 66.18; H, 4.33; N, 13.32. CV: one quasireversible wave at 0.56 V in the scan range 0.00 to +1.00 V.

Preparation of 3·2THF. The compound H_2DPAP (0.267 g, 1.00 mmol) was dissolved in 15 mL of THF and deprotonated at −78 °C by the addition of 2 equiv of MeLi (1.5 mL of 1.4 M MeLi in ether.) After the THF solution had slowly warmed to room temperature, it was transferred to a flask containing a mixture of $CrCl_2$ (0.10 g, 0.85 mmol) and tetrabutylammonium bromide (0.16 g, 0.50 mmol). The reaction mixture was stirred for 2 h at room temperature and then refluxed overnight. After cooling, the solvent was removed under vacuum and the remaining solid was washed with 2×20 mL of ether and 20 mL of a 10:1 ether−THF solution. The remaining solid was redissolved in THF and layered with hexanes. Dark red crystals formed after 6 days. Yield: 0.144 g (25%) Anal. Calcd for $C_{100}H_{126}N_{14}Cr_3$: C, 71.40; H, 7.67; N, 11.66. Found: C, 71.81; H, 7.62; N, 11.46. CV: one quasireversible wave at 0.03 V with scanning between −0.50 and 0.40 V, which is likely to correspond to oxidation of the separated Cr^{II} atom (see structure) to Cr^{III}. In the extended scan range −0.5 to 1.4 V, three irreversible peaks were seen at +0.03, 0.69, and 1.08 V.

Preparation of 4·2THF. The compound H_2DPAP (0.267 g, 1.00 mmol) was dissolved in 15 mL of THF and deprotonated at −78 °C with 2 equivalents of MeLi (1.5 mL of 1.4 M MeLi in ether.) After the THF solution had slowly warmed to room temperature, it was transferred into a flask which contained $NiCl_2$ (0.11 g, 0.85 mmol) and tetrabutylammonium bromide (0.16 g, 0.50 mmol). The reaction mixture was stirred for 2 h at room temperature and then refluxed overnight. After cooling, the solvent was removed under vacuum. The dark red solid was washed with 2×20 mL of ether and 20 mL of a 10:1 ether−THF solution and then dissolved in THF and layered with hexanes. Dark-red crystals were obtained after 5 days. Yield: 0.268 g (56%). ^1H NMR (300 MHz, CD_3CN, δ): 8.54 (d, 16H), 8.39 (t, 4H), 8.26 (t, 16), 7.96 (t, 8H), 7.24 (d, 8H), 2.92 (t, 16H), 2.55(q, 16H),

(8) Cotton, F. A.; Norman, J. G., Jr. *J. Coord. Chem.* **1971**, *1*, 161.
(9) Klinga, M.; Polama M.; Leskela, M. *Acta Crystallogr*. **1994**, *C50*, 2051.

Table 1. Crystal Data and Structure Refinement

	1·toluene	**1**·C_6H_{14}	**2**·toluene	**3**·2THF	**4**·2THF
empirical formula	$C_{75}H_{64}Cr_2N_{12}$	$C_{74}H_{70}Cr_2N_{12}$	$C_{75}H_{64}Mo_2N_{12}$	$C_{108}H_{140}Cr_3N_{14}O_2$	$C_{108}H_{140}N_{14}Ni_3O_2$
fw	1237.38	1231.42	1325.26	1822.34	1842.47
space group	$P2_1/n$	$C2/c$	$P2_1/n$	$C2/c$	$C2/c$
a, Å	10.460(1)	14.521(5)	10.601(2)	31.483(6)	31.729(2)
b, Å	32.32(4)	25.003(5)	32.432(2)	14.080(2)	13.7505(8
c, Å	18.798(1)	17.664(4)	18.809(4)	26.842(4)	27.167(2)
β, deg	105.94(2)	108.03(3)	106.149(9)	123.385(3)	125.104(1)
V, (Å^3)	6111(7)	6099(3)	6212(2)	9935(3)	9696(1)
Z	4	4	4	4	4
T, K	213(2)	213(2)	213(2)	213(2)	213(2)
ρ_{calc}, g/cm^{-3}	1.345	1.341	1.417	1.218	1.262
R1[a,c]/R1[a,d]	0.061/0.078	0.080/0.110	0.048/0.060	0.076/0.109	0.112/0.174
wR2[b,c]/wR2[b,d]	0.136/0.155	0.203/0.243	0.120/0.138	0.187/0.216	0.239/0.279

[a] $R1 = \sum||F_o| - |F_c||/\sum|F_o|$. [b] $wR2 = [\sum[w(F_o^2 - F_c^2)^2]/\sum[w(F_o^2)^2]]^{1/2}$; $w = 1/[^2(F_o^2) + (aP)^2 + bP]$, $P = [\max(F_o^2 \text{ or } 0) + 2(F_c^2)]/3$. [c] Denotes the value of the residual considering only the reflections with $I > 2\sigma(I)$. [d] Denotes the value of the residual considering all the reflections.

2.36 (m, 16H), 2.01 (t, 24H). Anal. Calcd for $C_{100}H_{128}N_{14}Ni_3$: C, 70.56; H, 7.58; N, 11.52. Found: C, 70.20; H, 7.68; N,11.86. CV: no reversible or quasireversible waves between +0.1 and +1.2 V.

X-ray Crystallography. Crystals of **1**·toluene, **1**·C_6H_{14}, and **2**·toluene were used for data collection at 213 K on a Nonius FAST area detector system, utilizing the software MADNES.[10] Each crystal was mounted on a quartz fiber with a small amount of silicone grease and transferred to a goniometer head. Cell parameters for FAST data were obtained from an autoindexing routine and were refined using 250 strong reflections. Cell dimensions and Laue symmetry were confirmed by axial photography. All data were corrected for Lorentz and polarization effects.

Data for **3**·2THF and **4**·2THF were collected on a Bruker SMART 1000 CCD area detector system. Cell parameters were obtained using SMART[11] software. Data were corrected for Lorentz and polarization effects using the program SAINTPLUS.[12] Absorption corrections were applied using SADABS.[13]

The positions of the heavy atoms were found by the direct methods program in SHELXS-97.[14] Subsequent cycles of least-squares refinement followed by difference Fourier syntheses revealed the positions of the non-hydrogen atoms. All aromatic hydrogen atoms were added in idealized positions. The hydrogen atoms attached to N were refined for $Cr_2(HDPAP)_4$ and $Mo_2(HDPAP)_4$.

Results and Discussion

Synthetic Considerations. The ligand precursor, H_2BPAP, can be made easily according to

2,6-dibromopyridine + 2PhNH$_2$·HCl →
2,6-bis(phenylamino)pyridine + 2HCl + 2HBr

Aniline hydrochloride must be present in great excess in order to obtain a satisfactory yield because it readily sublimes during the reaction. The analytically pure compound can be obtained by recrystallization of the crude product from an ethanol−water mixture. An additional recrystallization from a mixture of ethyl acetate and hexanes is necessary to obtain anhydrous crystals. Elemental analysis and ^{1}H NMR indicated that the purity was satisfactory. The ligand is fairly soluble in organic solvents, such as ether and hexane.

Table 2. Selected Bond Lengths (Å) and Angles (deg) for $Cr_2(HDPAP)_4$·toluene[a]

Cr(1)−Cr(2)	1.873(2)	Cr(1)···N(7)	3.148(5)
Cr(1)−N(11)	2.043(4)	Cr(1)−N(6)	2.063(3)
Cr(1)−N(9)	2.065(4)	Cr(2)−N(5)	2.039(3)
Cr(2)−N(8)	2.045(4)	Cr(2)−N(10)	2.071(4)
Cr(2)−N(1)	2.088(4)	Cr(1)−N(2)	2.027(4)
Cr(1)···N(12)	3.136(4)	Cr(1)···N(3)	3.066(5)
Cr(2)···N(4)	3.110(4)		
Cr(2)−Cr(1)−N(2)	99.2(1)	Cr(2)−Cr(1)−N(11)	99.3(1)
N(2)−Cr(1)−N(11)	161.4(1)	Cr(2)−Cr(1)−N(6)	92.8(1)
N(2)−Cr(1)−N(6)	90.4(1)	N(11)−Cr(1)−N(6)	89.1(1)
Cr(2)−Cr(1)−N(9)	92.8(1)	N(2)−Cr(1)−N(9)	87.1(1)
N(11)−Cr(1)−N(9)	91.6(1)	N(6)−Cr(1)−N(9)	174.2(1)
Cr(1)−Cr(2)−N(5)	98.7(1)	Cr(1)−Cr(2)−N(8)	98.6(1)
N(5)−Cr(2)−N(8)	162.8(1)	Cr(1)−Cr(2)−N(10)	92.2(1)
N(5)−Cr(2)−N(10)	89.1(1)	N(8)−Cr(2)−N(10)	89.8(1)
Cr(1)−Cr(2)−N(1)	92.1(1)	N(5)−Cr(2)−N(1)	89.1(1)
N(8)−Cr(2)−N(1)	90.7(1)	N(10)−Cr(2)−N(1)	175.6(1)
C(7)−N(1)−Cr(2)	118.9(3)	C(1)−N(1)−Cr(2)	124.1(3)

[a] The Cr−Cr distances are 1.875(2) in **1**·C_6H_{14}. All other interatomic distances are also similar to those for **1**·toluene.

The compound H_2BPAP has two N−H groups, each of which can be sequentially deprotonated by methyllithium to give the corresponding mono- and dianion. The second K_a is very small, and weaker deprotonating agents such as K^+OBu^- will not eliminate the second proton. For example, when 2 equiv of K^+OBu^- was added to 1 equiv of H_2BPAP along with $CrCl_2$ and TBA^+ in THF, under reflux conditions, the red orange dinuclear compound **1** was the only isolated product. The formation of the trinuclear chromium compound **3** required the use of MeLi; **3** is extremely sensitive to moisture, and it is slowly decomposed by CH_2Cl_2. Single crystals containing the trinuclear anion were obtained only after the addition of the large tetrabutylammonium counterion.

Structures of the Dinuclear Compounds. Two crystal forms of compound **1**, namely, **1**·toluene and **1**·C_6H_{14}, were obtained by slow diffusion of hexanes into the corresponding solutions of **1** in toluene and THF. Crystal data and structure refinement parameters are listed in Table 1, and some important bond distances and angles are shown in Table 2. The idealized D_{2d} core structure in the two crystals is essentially the same, having a metal−metal bonded dichromium unit with each chromium atom surrounded by nitrogen atoms. If the phenyl groups are neglected, the structure is essentially eclipsed as shown in Figures 1 and 2. The Cr−Cr distances of 1.873(2) Å in **1**·toluene and 1.875(2) Å in **1**·C_6H_{14} are similar to that, 1.870(3) Å, in

(10) Pflugrath, J.; Messerschmitt, A. *MADNES*, Munich Area Detecor (New EEC) System, Version EEC 11/1/89, with enhancement by Enraf-Nonius Corp., Delft, The Netherlands. A description of MADNES appears: Messerschmitt, A.; Pflugrath, J. *J. Appl. Crystallogr.* **1987**, *20*, 306.
(11) *SMART V5.05 Software for the CCD Detector System*; Bruker Analytical X-ray Systems, Inc.: Madison, WI, 1998.
(12) *SAINTPLUS V5.05 Software for the CCD Detector System*; Bruker Analytical X-ray Systems, Inc.: Madison, WI, 1998.
(13) *SADABS*. Program for absorption correction using SMART CCD based on the method of Blessing: Blessing, R. H. *Acta Crystallogr.* **1995**, *A51*, 33.
(14) Sheldrick, G. M. *Acta Crystallogr.* **1990**, *A46*, 467.

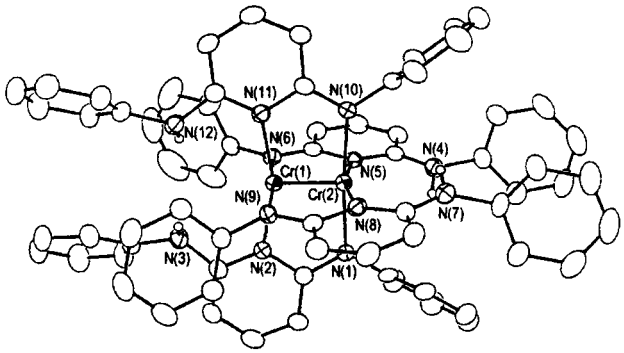

Figure 1. Perspective view of $Cr_2(HBPAP)_4$ in **1**·toluene. Atoms are drawn at the 40% probability level, and aromatic hydrogen atoms are omitted for clarity.

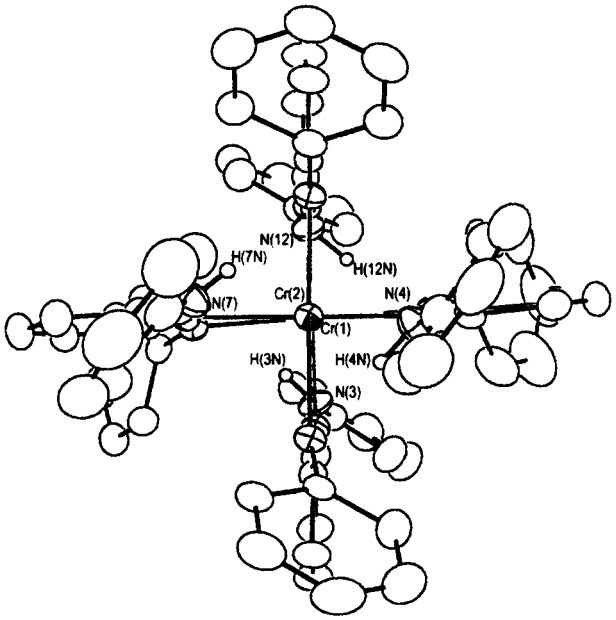

Figure 2. A view down the Cr−Cr vector in **1**·toluene.

Cr_2(6-Me-2-$NHC_6H_3N)_4$, where the ligand is very similar to the coordinated part of HBPAP.[15] However, the Cr−Cr distance is very short when compared with those in other dichromium compounds with somewhat similar tridentate nitrogen ligands. For example, the distances between chromium atoms in Cr_2(DPhIP)·2THF (DPhIP is the anion of 2,6-di(phenylimino)-piperidine) and $Cr_2(dpa)_4$ are 2.155(1) Å and 1.943(2) Å, respectively.[7] While the average distance of 3.114[4] Å[16] from a pendent N to a metal atom in **1** is not much greater than the corresponding distances of 2.901[3] Å[16] and 2.920[6] Å[16] in $Cr_2(DPhIP)_4$·2THF and $Cr_2(dpa)_4$, respectively,[7] there is a significant chemical difference between these ligands. Because of the sp^3 hybridization and the proton present in the anilido nitrogen atom in $Cr_2(HBPAP)_4$, the donor ability of the pendent N atom from the anilido group is far inferior to that of the sp^2 N atoms found at the axial positions of $Cr_2(DPhIP)_4$ and $Cr_2(dpa)_4$. Thus the dichromium distance in $Cr_2(HDPAP)_4$ falls into the typical range of dichromium quadruple bonds.

The dimolybdenum complex, **2**·toluene, is isomorphous to the dichromium complex, **1**·toluene, and, as shown in Figure 3, the molecular structure is very similar. The Mo−Mo distance of 2.0813(5) Å is typical of a quadruply bonded Mo_2 unit (Table 3). The Mo−Mo and Mo−N distances and the angles in the metal core are very similar to those found in $Mo_2(PhNPy)_4$,[17] where PhNPy stands for the anion of 2-anilinopyridine.

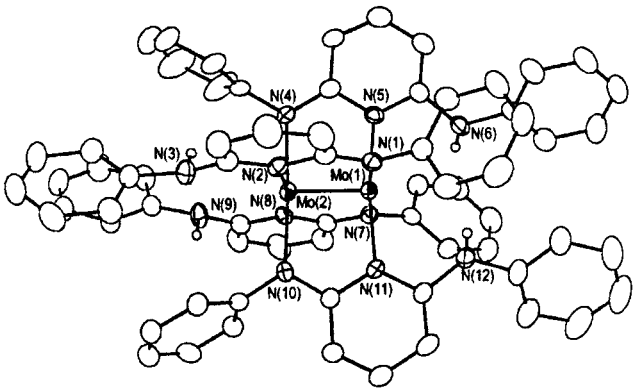

Figure 3. Perspective view of $Mo_2(HBPAP)_4$ in **2**·toluene. Atoms are drawn at the 40% probability level, and aromatic hydrogen atoms are omitted for clarity.

Table 3. Selected Bond Lengths (Å) and Angles (deg) for $Mo_2(HDPAP)_4$·toluene

Mo(1)−Mo(2)	2.0813(5)	Mo(2)−N(10)	2.153(4)
Mo(1)−N(5)	2.137(4)	Mo(2)−N(8)	2.137(4)
Mo(1)−N(11)	2.148(4)	Mo(2)−N(2)	2.143(4)
Mo(1)−N(1)	2.174(4)	Mo(2)−N(4)	2.144(4)
Mo(1)−N(7)	2.178(4)		
Mo(2)−Mo(1)−N(5)	94.1(1)	N(5)−Mo(1)−H(7N)	55.1(1)
Mo(2)−Mo(1)−N(11)	94.01(9)	N(11)−Mo(1)−H(7N)	117.4(1)
N(5)−Mo(1)−N(11)	171.9(2)	N(1)−Mo(1)−H(7N)	105.6(1)
Mo(2)−Mo(1)−N(1)	90.8(1)	N(7)−Mo(1)−H(7N)	72.0(1)
N(5)−Mo(1)−N(1)	89.7(2)	Mo(2)−Mo(1)−H(9N)	145.1(1)
N(11)−Mo(1)−N(1)	89.8(2)	N(5)−Mo(1)−H(9N)	115.4(1)
Mo(2)−Mo(1)−N(7)	91.3(1)	N(11)−Mo(1)−H(9N)	56.8(1)
N(5)−Mo(1)−N(7)	88.9(2)	N(1)−Mo(1)−H(9N)	72.2(1)
N(11)−Mo(1)−N(7)	91.2(2)	N(7)−Mo(1)−H(9N)	106.6(1)
N(1)−Mo(1)−N(7)	177.5(1)	Mo(1)−Mo(2)−N(8)	94.5(1)

^{1}H NMR Studies of $Cr_2(HDPAP)_4$ and $Mo_2(HDPAP)_4$. The ^{1}H NMR spectra showed that the purity of **1** and **2** was good. All signals corresponding to the aromatic C−H protons were sharp, as expected from a diamagnetic species. However, the signals associated with the amine hydrogen atoms on each of the pendent N atoms were slightly broader and were found at 3.46 ppm for **1** and 3.04 ppm for **2**. The corresponding signal in the neutral H_2BPAP is at 8.04 ppm, and for the lithium salt of $HBPAP^-$ it is at 6.44 ppm. This displacement is significantly larger than that of the aromatic hydrogen atoms which change by less than 1 ppm from the neutral molecule to the monoanionic species to those of the metal−metal bound complexes. The small downfield displacement, 1.6 ppm, of the signals corresponding to the amine hydrogen atoms of the monoanionic species compared to that of the neutral one is not surprising and can be attibuted to the negative charge on the monoanion as well as possible pairing of ions by formation of intermolecular hydrogen bonds between N−H units and deprotonated nitrogen atoms in the monoanionic species, as shown in Scheme 3. The much greater displacement of the N−H signals of **1** and **2** toward higher field is quite remarkable. When compared to those of LiHBPAP, these signals are displaced by 2.98 and 3.40 ppm upfield for **1** and **2**, respectively. There are many previous examples of relatively large shifts in the opposite direction. For example, the methine hydrogen atoms of bridging formamidinate groups, ArN−C(H)−NAr, in $M_2(DArF)_4$ complexes are well

(15) Cotton, F. A.; Niswander, R. H.; Sekutowski, J. C. *Inorg. Chem.* **1978**, *17*, 3541.
(16) Numbers within square brackets are associated with average values.
(17) Chakravarty, A. R.; Cotton, F. A.; Shamshoum, E. S. *Inorg. Chem.* **1984**, *23*, 4216.

Scheme 3

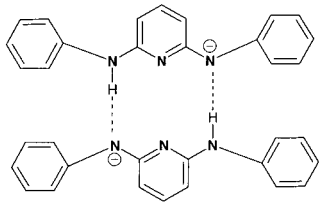

documented[18] for compounds containing M−M multiple bonds. These signals are found at ca. 8.53 ppm in quadruply bonded dimolybdenum complexes and at ca. 6.28 ppm in the corresponding nonmetal−metal bound dinickel complexes.[18] Familiar also are the differences of ca. 1 ppm observed for proximal and distal protons in complexes of the type $M_2Cl_4(PR)_4$,[19] $M_2Cl_4(diphos)_2$,[20] or $M_2(NR_2)_6$[21] where again there are metal−metal bonds.

High- and low-field displacements share a common origin. In a semiclassical way, the angular momentum of electrons in the M−M multiple bond about the bond axis induces a magnetic field which is highly anisotropic. This magnetic anisotropy has also been found in many organic compounds and is mainly responsible for the significantly different shifts found in benzene and alkyne systems. For example, in acetylene the protons have signals at δ 2.35 ppm, more shielded than those in ethylene (δ 4.60 ppm).[22] In acetylene, the triple bond is along the molecular axis. When this axis is aligned with the applied magnetic field, the circulation of the π-electrons of the bond gives rise to an opposing magnetic field and the NMR peak is found further upfield than that predicted from electronegativity considerations alone. Clearly, similar behavior must occur for triple and quadruple bonds between metal atoms.

For metal−metal multiply bound systems, the theoretical considerations of McConnell[23] can be used to explain long-range shielding or deshielding. This simple mathematical model relates the chemical shift change, $\Delta\delta$, and the molar diamagnetic anisotropy, χ. The magnitude of the magnetic anisotropy, given by the difference between the parallel and perpendicular components along the metal−metal bond, has been demonstrated[18] to be correlated to the chemical shift of a given hydrogen atom by the following equation:

$$\Delta\chi = \chi_{\parallel} - \chi_{\perp} = \frac{12\pi R^3 \Delta\delta}{1 - 3\cos^2\theta}$$

where R is the length of the vector from the center of the bond to the proton in question (e.g., the N−H proton on the hanging N atom of a ligand in **1** and **2**) and θ is the angle subtended by R and the M−M axis. The value $\Delta\delta$ is the displacement of the resonance from where it would be in the absence of the anisotropy. Because of the angular dependence of this relationship, the value of the function for an axially symmetrical bond changes sign at 55° 44′. Thus one would expect protons above the M−M bond to be deshielded (e.g., the methine protons of a formamidinate ligand) and thus shifted downfield, or shielded if they are more or less along the M−M axis, as shown schematically in Figure 4 and thus shifted upfield. Since the amine protons in **1** and **2** fall in the positive shielding zone, one would expect an upfield displacement, relative to that of the noncoordinated ligands, exactly as observed here. To our knowledge, this is the first time an upfield displacement has been documented in the chemistry of multiply bonded complexes.

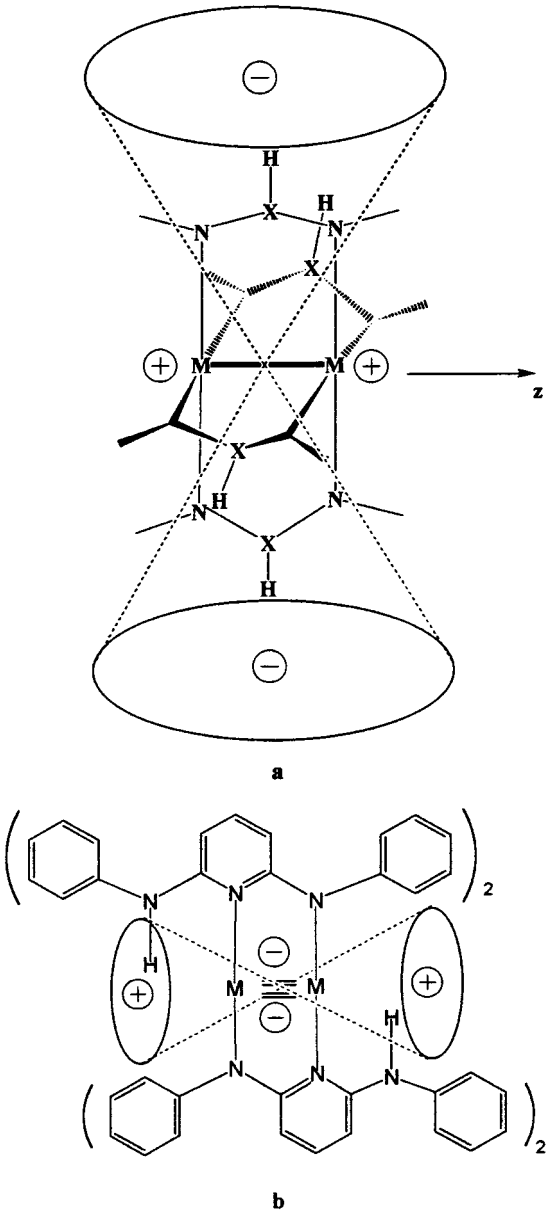

Figure 4. Shielding and deshielding caused by magnetic anisotropy of the M−M multiple bond in dinuclear paddlewheel compounds. Positive signs (+) indicate shielding zones, while negative signs (−) represent deshielding zones.

Using the above equation, many calculations have been performed[18] using the methine protons as probes for metal−metal bonded paddlewheel compounds having four formamidinate ligands. For these rigid groups, the angle θ is essentially 90° and the distance R is easily calculated using the structural parameters. Such calculations have, therefore, been very successful in correlating the ^{1}H NMR chemical shifts with structure

(18) See, for example: (a) Cotton, F. A.; Ren, T. *J. Am. Chem. Soc*. **1992**, *114*, 2237. (b) Lin, C.; Protasiewicz, J. D.; Smith, E. T.; Ren, T. *Inorg. Chem.* **1996**, *35*, 6422. (c) Cotton, F. A.; Daniels, L. M.; Murillo, C. A. *Angew. Chem., Int. Ed. Engl.* **1992**, *31*, 737.
(19) San Filippo, J., Jr. *Inorg. Chem.* **1972**, *11*, 3140.
(20) See, for example: (a) Cotton, F. A.; Kitagawa, S. *Polyhedron* **1988**, *18*, 1673. (b) Cotton, F. A.; Kitagawa, S. *Inorg. Chem.* **1987**, *26*, 3463.
(21) See, for example: Chisholm, M. H.; Cotton, F. A.; Frenz, B. A.; Reichert, W. W.; Shive, L. W.; Stults, B. R. *J. Am. Chem. Soc.* **1976**, *98*, 4469.
(22) Silverstein, R. M.; Bassler, G. C.; Morrill, T. C. *Spectrometric Identification of Organic Compounds*, 4th ed.; John Wiley & Sons: New York, 1981.
(23) McConnell, H. N. *J. Chem. Phys.* **1957**, *27*, 226. See also refs 17−20.

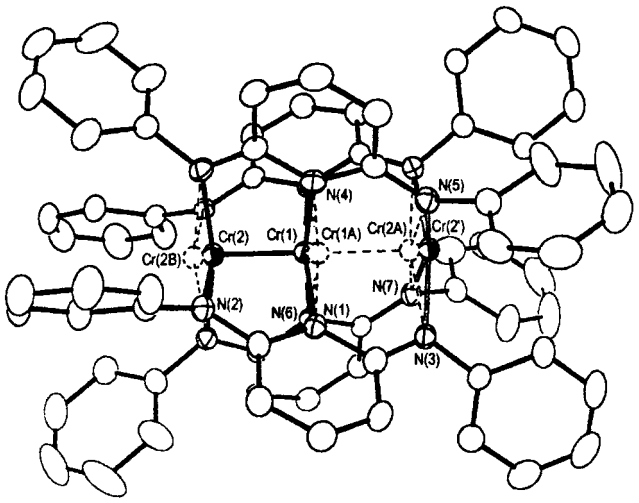

Figure 5. Perspective view of $Cr_3(BPAP)_4^{2-}$ in **3**·THF. Atoms are drawn at the 40% probability level, and hydrogen atoms are omitted for clarity. One set of disordered chromium atoms is represented by broken circles.

for the formamidinate compounds, and quantitative estimates of the diamagnetic anisotropies have been made. Unfortunately for the $M_2(HBPAP)_4$ compounds **1** and **2**, this type of calculation is not reliable. One could obtain all the necessary values from the solid state structure, but since the N−H groups of the pendent HBPAP ligand are not restrained to fixed positions in solution,[24] no correlation between the solid state and the solution structures, in this respect, is possible.

Structures of Compounds 3 and 4. Compound **3** crystallized in the space group *C*2/*c* with two interstitial THF molecules. Here, a linear chain of three chromium atoms is surrounded by four BPAP dianions, as shown in Figure 5. The trinuclear anion resides on a crystallographic site of 2-fold symmetry with the 2-fold axis perpendicular to the Cr−Cr−Cr chain. However, the trinuclear chromium chain is actually very unsymmetrical. The initial appearance of equality of the Cr−Cr distances is due to crystallographic disorder. This type of disorder has been encountered also in other species containing linear Cr_3^{6+} cores.[1b] Full anisotropic refinement of the chromium atoms in the chain was not possible because of disorder, but the two Cr to Cr distances were found to be quite different, namely, 1.904(3) Å for Cr(1)−Cr(2) and 2.589(3) Å for Cr(1)−Cr(2′) (Table 4). Therefore, the bonding in this trinuclear chromium chain should be considered to consist of a Cr−Cr quadruple bond and an isolated Cr^{II} unit, with the latter having approximately square planar geometry. The countercations, $Bu^n{}_4N^+$, reside on general positions in the unit cell.

Figure 6 shows an end view of the trinuclear anion of **3**. The torsion angle N(2)···Cr(2)···Cr(1)···(N1) is 15.3°; the total torsion angle in the molecule is 30.6°. This is smaller than that in the similar trinuclear dpa complex (45.4°).[1e] Thus, the idea that simply eliminating H···H interactions such as those in the dpa anion (Scheme 1a) would produce a trinuclear species without a torsion angle did not prove correct. The reason for this is not readily evident. We hope to address this problem in the future by employing molecular mechanics calculations.

The trinuclear nickel compound, **4**·2THF, is isomorphous with **3**·2THF, crystallizing in space group *C*2/*c*, with $Z = 4$.

(24) Furthermore, the value of $\Delta\delta$ for $M_2(formamidinate)_4$ complexes is typically obtained from the chemical shifts of the metal−metal bound complex and the analogous nonmetal−metal bound $Ni_2(formamidinate)_4$ complex. So far we have been unable to prepare a nickel analogue of the $M_2(HBPAP)_4$, M = Cr and Mo.

Table 4. Selected Bond Lengths (Å) and Angles (deg) for $(TBA)_2Cr_3(BPAP)_4$·THF[a,b]

Cr(1)−Cr(2)	1.904(3)	Cr(2′)···Cr(1)	2.589(2)
Cr(1)−N(1A)	2.050(4)	Cr(2′)−N(2A)	2.031(6)
Cr(1)−N(4)	2.059(4)	Cr(2′)−N(7)	2.044(4)
Cr(1)−N(6)	2.062(4)	Cr(2′)−N(3)	2.071(6)
Cr(1)−N(1)	2.082(4)	Cr(2′)−N(5)	2.076(4)
Cr(2)−N(3A)	2.029(6)	Cr(2)−N(2)	2.071(6)
Cr(2)−N(5A)	2.036(4)	Cr(2)−N(7A)	2.079(4)

Cr(2)−Cr(1)−N(1A)	94.0(2)	N(6)−Cr(1)−N(1)	88.8(1)
Cr(2)−Cr(1)−N(4)	93.47(8)	Cr(1)−Cr(2)−N(3A)	95.6(2)
N(1A)−Cr(1)−N(4)	90.7(1)	Cr(1)−Cr(2)−N(5A)	95.9(1)
Cr(2)−Cr(1)−N(6)	94.00(8)	N(3A)−Cr(2)−N(5A)	90.9(2)
N(1A)−Cr(1)−N(6)	89.7(1)	Cr(1)−Cr(2)−N(2)	95.8(2)
N(4)−Cr(1)−N(6)	172.7(1)	N(3A)−Cr(2)−N(2)	168.4(2)
Cr(2)−Cr(1)−N(1)	93.4(2)	N(5A)−Cr(2)−N(2)	89.7(2)
N(1A)−Cr(1)−N(1)	172.5(1)	Cr(1)−Cr(2)−N(7A)	95.0(1)
N(4)−Cr(1)−N(1)	89.8(1)	N(3A)−Cr(2)−N(7A)	89.6(2)
N(5A)−Cr(2)−N(7A)	169.0(2)	N(3)−Cr(2′)−N(5)	88.7(2)
N(2)−Cr(2)−N(7A)	87.6(2)	N(2A)−Cr(2′)−N(7)	89.6(2)
N(2A)−Cr(2′)−N(5)	89.7(2)	N(2A)−Cr(2′)−N(3)	168.1(2)
N(7)−Cr(2′)−N(5)	167.6(2)	N(7)−Cr(2′)−N(3)	89.4(2)

[a] Atomic labels with the prime symbol (′) denote the disordered atom counterparts of the unprimed atoms. [b] Atomic labels with "A" denote symmetry-related atoms.

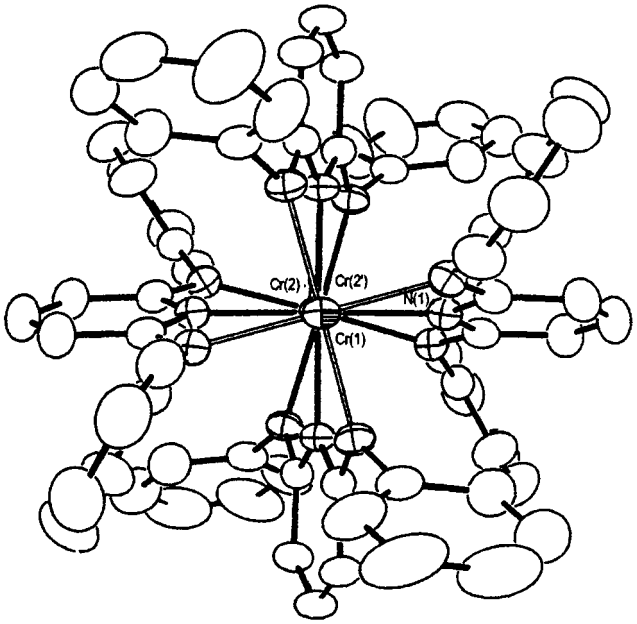

Figure 6. A view looking down the Cr_3 unit in **3**·THF.

The anion therefore has crystallographic symmetry C_2, and in this case the metal atom chain is symmetrical; there is no disorder. Again, there is no axial ligation and there is an overall twist of about 30°. The structure is depicted in Figure 7, and metrical parameters are listed in Table 5. The end nickel atoms as well as the central one are coordinated by an essentially square planar array of nitrogen atoms, and the Ni−N distances to the end nickel atoms, with an average value of 1.917[6] Å,[16] are scarcely different from those to the central nickel atom, 1.906[6] Å.[16] From this structure it would be expected that all three nickel atoms would be in a low-spin (i.e., diamagnetic) state, and this is indeed the case as shown by the ^1H NMR spectrum.

The two Ni···Ni separations are 2.368(1) Å, which is much shorter than those in $Ni_3(dpa)_4Cl_2$,[1f] 2.433[8] Å.[16] However, in $Ni_3(dpa)_4Cl_2$ as well as in all nickel compounds in this class with more extended chains,[25] i.e., Ni_5, Ni_7, Ni_9, the nickel atoms at the ends are different from those inside the chain. The end

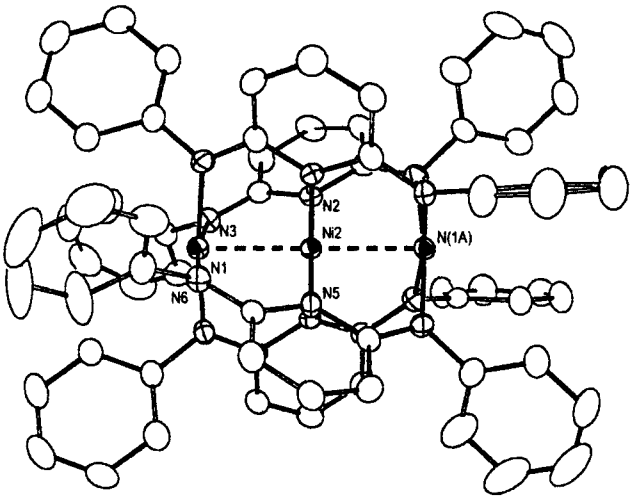

Figure 7. Perspective view of the anion $Ni_3(BPAP)_4^{2-}$ in **4**·THF. Atoms are drawn at the 40% probability level, and aromatic hydrogen atoms are omitted for clarity.

Table 5. Selected Interatomic Separations (Å) and Angles (deg) for $(TBA)_2Ni_3(BPAP)_4$·THF[a]

Ni(2)···Ni(1)	2.368(1)		
Ni(2)−N(6)	1.897(8)	Ni(1)−N(3A)	1.916(5)
Ni(2)−N(4)	1.907(7)	Ni(1)−N(7)	1.917(5)
Ni(2)−N(2)	1.910(5)	Ni(1)−N(5)	1.919(6)
Ni(2)−N(2A)	1.910(5)	Ni(1)−N(1)	1.919(5)
N(6)−Ni(2)−N(4)	180.00(1)	N(2A)−Ni(2)···Ni(1)	90.1(2)
N(6)−Ni(2)−N(2)	89.8(2)	Ni(1A)−Ni(2)···Ni(1)	179.93(7)
N(4)−Ni(2)−N(2)	90.2(2)	N(3A)−Ni(1)−N(7)	90.8(2)
N(6)−Ni(2)−N(2A)	89.8(2)	N(3A)−Ni(1)−N(5)	88.9(2)
N(4)−Ni(2)−N(2A)	90.2(2)	N(7)−Ni(1)−N(5)	173.0(2)
N(2)−Ni(2)−N(2A)	179.5(3)	N(3A)−Ni(1)−N(1)	173.1(2)
N(6)−Ni(2)···Ni(1A)	90.04(4)	N(7)−Ni(1)−N(1)	89.0(2)
N(4)−Ni(2)···Ni(1A)	89.96(4)	N(5)−Ni(1)−N(1)	90.5(2)
N(2)−Ni(2)···Ni(1A)	90.1(2)	N(3A)−Ni(1)···Ni(2)	86.6(2)
N(2A)−Ni(2)···Ni(1A)	89.9(2)	N(7)−Ni(1)···Ni(2)	86.4(2)
N(6)−Ni(2)···Ni(1)	90.04(4)	N(5)−Ni(1)···Ni(2)	86.5(2)
N(4)−Ni(2)···Ni(1)	89.96(4)	N(1)−Ni(1)···Ni(2)	86.5(2)

[a] Atomic label with "A" denotes the symmetry-related atom unit.

nickel atoms have a fifth ligand atom (e.g., Cl^-, NCS^-) and are high spin. Thus, while the inner nickel atom(s) is (are) square-planar, low-spin atoms with relatively short (ca. 1.90 Å) Ni−N bonds, those on the ends are five-coordinate, high-spin atoms, with longer Ni−N bonds (ca. 2.1 Å) and the Ni···Ni separations to the terminal nickel atoms are long. It is the absence of axial ligation in the present case leading to the end nickel atoms being square-planar, low-spin atoms that allows for their closer approach to the central nickel atom.

Scheme 4

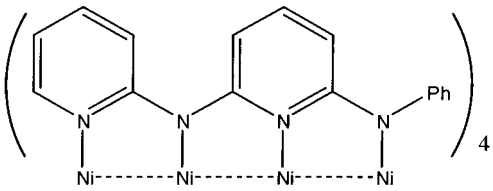

Compound **4** is not the first compound with a chain of nickel atoms having no axial ligation. The compound shown in Scheme 4 was reported in 1999.[25b] It is diamagnetic, like **4**, but has Ni···Ni separations that are appreciably shorter than those in **4**, namely, 2.3269[6], 2.3010[6], and 2.3280[6] Å,[16] as compared to 2.368(1) Å in **4**. The Ni−N distances in both this compound and **4** are quite similar, all being in the range 1.90−1.93 Å. It seems clear that unless there are axial ligands present, chains of nickel(II) atoms simply consist of stacked square, diamagnetic NiN_4 units. In both compounds the stacks are twisted, however.

Conclusions

It has been shown that the potentially tridentate ligands, $BPAP^{2-}$, can do two things: (1) remain as $HBPAP^-$ and bind only a pair of metal ions (Cr_2^{4+}, Mo_2^{2+}) locked into a strong quadruply bonded pair, or (2) support a chain of three metal ions (Cr_3^{6+}, Ni_3^{6+}). In the first case, what distinguishes $M_2(HBPAP)_4$ compounds from previous cases where potentially tridentate ligands have formed only binuclear compounds (for example, $Cr_2(DPhIP)_4$ and $Cr_2(dpa)_4$) is that in the $M_2(HBPAP)_4$ compounds there are no significant axial interactions to cause lengthening of the M_2 bond. Importantly, an upfield displacement caused by the magnetic anisotropy of the quadruple bonds was observed for this first time in the NMR spectra of compounds **1** and **2**. In the case of the $M_3(BPAP)_4^{2-}$ ions, there are, again, no axial interactions because these anionic species do not attract ligands. This results in their having different properties from the $M_3(dpa)_4X_2$ molecules. Most notably, the $Ni_3(BPAP)_4^{2-}$ ion is diamagnetic and all three nickel ions can be described as square-planar, low-spin Ni^{II} centers.

Efforts are underway to make compounds containing $M_3(BPAP)_4^{2-}$ ions with other metal atoms.

Acknowledgment. We gratefully acknowledge financial support from the National Science Foundation.

Supporting Information Available: X-ray crystallographic files in CIF format for compounds **1**−**4**. This material is available free of charge via the Internet at http://pubs.acs.org.

IC001376G

(25) (a) Wang, C. C.; Lo, W. C.; Chou, C. C.; Lee, G. H.; Chen, J. M.; Peng, S. M. *Inorg. Chem.* **1998**, *37*, 4059. (b) Lai, S. Y.; Lin, T. W.; Chen, Y. H.; Wang, C. C.; Lee, G. H.; Yang, M. K.; Leung, M. K.; Peng, S. M. *J. Am. Chem. Soc.* **1999**, *121*, 250.